

CMC TORI OF REVOLUTION IN \mathbb{S}^3 : ADDITIONAL DATA ON THE SPECTRA OF THEIR JACOBI OPERATORS

WAYNE ROSSMAN AND NAHID SULTANA

ABSTRACT. We prove a theorem about elliptic operators with symmetric potential functions, defined on a function space over a closed loop. The result is similar to a known result for a function space on an interval with Dirichlet boundary conditions. These theorems provide accurate numerical methods for finding the spectra of those operators over either type of function space. As an application, we numerically compute the Morse index of constant mean curvature tori of revolution in the unit 3-sphere \mathbb{S}^3 , confirming that every such torus has Morse index at least five, and showing that other known lower bounds for this Morse index are close to optimal.

1. INTRODUCTION

Our goal is to study the Morse index of constant mean curvature (CMC) tori of revolution in the spherical 3-space \mathbb{S}^3 , where the Morse index is the number of negative eigenvalues of the Jacobi operators of those surfaces. The central tool we use is a result about the number of nodes of eigenfunctions of those Jacobi operators. The result, proven with the standard Sturm comparison technique in ordinary differential equations and closely related to classically known results, is proven here before being applied to the index of CMC surfaces of revolution in \mathbb{S}^3 . So let us start by considering an operator of the form

$$\mathcal{L} = -\frac{d^2}{dx^2} - V, \quad \text{i.e. } \mathcal{L}(f) = -\frac{d^2}{dx^2}f - V \cdot f,$$

on function spaces \mathcal{F}_p over a closed loop or \mathcal{F}_0 over an interval $[0, a]$ with Dirichlet boundary conditions:

$$\begin{aligned} \mathcal{F}_p &= \mathcal{F}_p(a) = \{f : \mathbb{R} \xrightarrow{C^\infty} \mathbb{R} \mid f(x) = f(x+a)\}, \\ \mathcal{F}_0 &= \mathcal{F}_0(a) = \{f : [0, a] \xrightarrow{C^\infty} \mathbb{R} \mid f(0) = f(a) = 0\}, \quad a > 0. \end{aligned}$$

We assume the potential function $V = V(x)$ is real-valued and real-analytic on the closed interval $[0, a]$, and $V \in \mathcal{F}_p$ when the function space \mathcal{F}_p is used. However, we do not assume V is in \mathcal{F}_0 when the function space \mathcal{F}_0 is used, that is, we do not assume $V(0)$ and $V(a)$ are zero.

The eigenvalue problem is to find $\lambda \in \mathbb{R}$ and $f \in \mathcal{F}_p$ (or \mathcal{F}_0) that solve the second-order ordinary differential equation (ODE)

$$(1.1) \quad \mathcal{L}(f) = \lambda f.$$

The operator $-\mathcal{L}$ is elliptic and it is well-known ([2], [3], [12], [19]) that the eigenvalues of \mathcal{L} are real and form a discrete sequence

$$\lambda_1 < \lambda_2 \leq \lambda_3 \leq \dots \uparrow +\infty$$

(each considered with multiplicity 1) whose first eigenvalue λ_1 is simple. The eigenvalues form a discrete spectrum, and corresponding eigenfunctions

$$f_1, f_2, f_3, \dots \text{ in } \mathcal{F}_p \text{ or in } \mathcal{F}_0, \quad \mathcal{L}(f_j) = \lambda_j f_j,$$

can be chosen to form an orthonormal basis with respect to the standard L^2 norm on \mathcal{F}_p or \mathcal{F}_0 over $[0, a]$.

Let

$$\Sigma_p = \mathbb{R}/(x \sim x+a) \quad \text{and} \quad \Sigma_0 = [0, a]$$

denote the domains of the functions in \mathcal{F}_p and \mathcal{F}_0 , respectively. The *nodes* of an eigenfunction $f \in \mathcal{F}_p$ (or \mathcal{F}_0) are those points of Σ_p (or Σ_0) at which f vanishes. When f is not identically zero, the fact that \mathcal{L} is second-order and linear implies all zeros of f are isolated and of lowest order, i.e. if $f(0) = 0$, then $(\frac{d}{dx}f)(0) \neq 0$.

We have the following two theorems, the second of which uses a symmetry condition on V . The first theorem is well-known and can be proven using Sturm comparison and Courant's nodal domain theorem (see [5], [6], [7], [8], for example):

Theorem 1.1. *Consider the operator \mathcal{L} on the function space \mathcal{F}_0 of C^∞ functions over Σ_0 with Dirichlet boundary conditions. Then all eigenspaces are 1-dimensional, and to find a nonzero solution $f \in \mathcal{F}_0$ of $\mathcal{L}(f) = \lambda f$ for some eigenvalue λ , without loss of generality we may assume:*

$$f(0) = 0 \quad , \quad \left(\frac{d}{dx}f\right)(0) = 1 \quad .$$

Furthermore, any eigenfunction associated to the j 'th eigenvalue λ_j of \mathcal{L} has exactly $j + 1$ nodes.

The following theorem can be similarly proven, but is a bit more complicated, because in this case the eigenvalues are not always simple. We will prove Theorem 1.2 here (and in the process also prove Theorem 1.1). The conclusions about the initial conditions in these two theorems are quite trivial; it is the conclusions about the number of nodes of the eigenfunctions that are of the most interest to us.

Theorem 1.2. *Consider the operator \mathcal{L} on the function space \mathcal{F}_p of C^∞ periodic functions over Σ_p . Suppose the real-analytic function $V \in \mathcal{F}_p$ has the symmetry*

$$(1.2) \quad V(x) = V(-x) \quad \forall x \in \mathbb{R} \quad .$$

Let $\lambda_1 < \lambda_2 \leq \lambda_3 \leq \dots \uparrow +\infty$ be the spectrum of \mathcal{L} with a corresponding basis $f_1, f_2, f_3, \dots \in \mathcal{F}_p$ of eigenfunctions. Then the eigenspaces are each at most 2-dimensional, and to find a basis for the eigenspace associated to λ_j , we may assume:

- When the eigenspace for λ_j is 1-dimensional, we may take f_j so that one of

$$f_j(0) = 1 \quad , \quad \left(\frac{d}{dx}f_j\right)(0) = 0 \quad \text{or} \quad f_j(0) = 0 \quad , \quad \left(\frac{d}{dx}f_j\right)(0) = 1 \quad \text{holds.}$$

- When the eigenspace for λ_j is 2-dimensional, and $\lambda_j = \lambda_{j+1}$, we may take

$$f_j(0) = 1 \quad , \quad \left(\frac{d}{dx}f_j\right)(0) = 0 \quad \text{and} \quad f_{j+1}(0) = 0 \quad , \quad \left(\frac{d}{dx}f_{j+1}\right)(0) = 1 \quad .$$

Furthermore, any eigenfunction in \mathcal{F}_p associated to λ_j has exactly j nodes if j is even, and $j - 1$ nodes otherwise.

After proving these results in Section 2, we will see in Section 3 that Theorem 1.2 gives a method to numerically compute the spectra of the operator \mathcal{L} . Then, in Section 4, we apply that method to study the index of CMC surfaces of revolution in the round 3-sphere.

In [13], a method was given for computing the eigenvalues for the Jacobi operator of a Wente torus, involving the Rayleigh-Ritz method and restricting to finite dimensional subspaces of function spaces defined over tori. Then in [14], both this method and a second more direct method were given for computing the first eigenvalue of the Jacobi operator of a Delaunay surface with respect to periodic functions, and the second method depended on Delaunay surfaces being surfaces of revolution. It was argued in [14] that, although the second method was clearly the simpler of the two, the first method was still of value because it could compute any eigenvalue of the Jacobi operator, while the second method computed only the first eigenvalue. However, via Theorem 1.2, the second method in [14] in fact extends to a method that gives any eigenvalue and hence is both simpler and equally as robust as the first method. Additionally, this extended second method involves only using any standard ODE solver, such as the Euler algorithm or the Runge-Kutta algorithm, and so has only as much numerical error as those algorithms have, whereas the first method involves restrictions to finite dimension subspaces for which the numerical error cannot be easily estimated and appears to be very much larger than for the extended second method. (This can be seen by comparing the respective errors of the two methods in cases where the spectra are explicitly known.)

Certainly the first method was necessary in [13], because Wente surfaces are not surfaces of revolution. But for the above reasons, the method we give here is in every way superior to the methods found in [13] and [14], in the case of CMC surfaces of revolution.

A surface of revolution in the unit 3-sphere \mathbb{S}^3 is generated by revolving a given planar curve about a geodesic line in the geodesic plane containing this given curve. The given curve is called the profile curve and the geodesic line is called the axis of revolution. The profile curves of non-spherical non-flat CMC surfaces of revolution in \mathbb{S}^3 will periodically have minimal and maximal distances to the axis of revolution [9]. We call the points of minimal distance the *necks*, and the points of maximal distance the *bulges*. In general, when these surfaces close to become compact surfaces without boundary, they are of the following 3 types:

- *round spheres*, every point of which is the same distance from a fixed point (the center),
- *flat* CMC tori, every point of which is the same distance from a closed geodesic (the axis of revolution),
- *non-flat* CMC tori, where the distances from the axis of revolution to the necks and bulges are not equal.

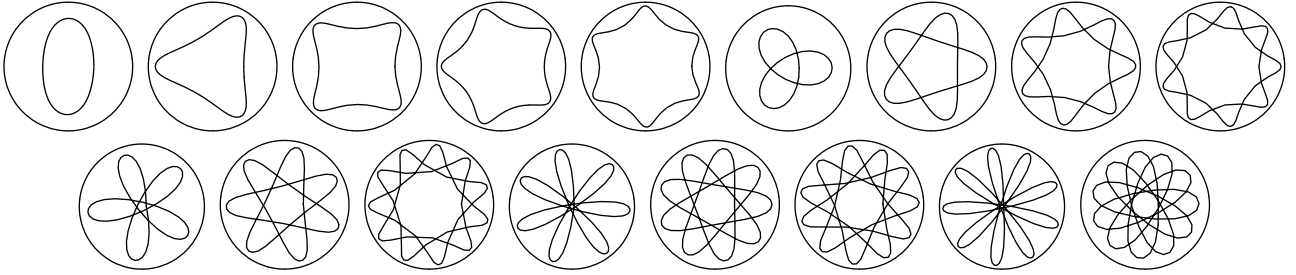


FIGURE 1. Profile curves for surfaces that we label U_i for $i = 1, 2, \dots, 17$ (U_1, \dots, U_9 from left to right in the upper row, U_{10}, \dots, U_{17} from left to right in the lower row). These are profile curves of CMC tori of revolution, shown in totally geodesic hemispheres having the rotation axis as boundary. The images are stereographic projections from \mathbb{S}^3 to $\mathbb{R}^3 \cup \{\infty\}$. The outer circle is the rotation axis, with profile curve inside. All of these surfaces are unduloidal, in the sense that the projections of these curves to the nearest points in the rotation axis are everywhere continuous local injections.

Because these surfaces are closed, the number of negative eigenvalues of their Jacobi operators, counted with multiplicity and called the *Morse index*, is finite. The Morse index is of interest because it is a measure of the degree of instability of the surface. In the first two cases above, the Morse index is easily explicitly computed [16], being 1 for the first case (this is closely related to the fact that spheres are stable [1]) and always at least 5 for the second case. Regarding the third case, the authors proved the following in [16]:

Theorem 1.3. *Let \mathcal{S} be a non-flat closed CMC torus of revolution in \mathbb{S}^3 , with k bulges and k necks. Let w denote the wrapping number of the projection of a profile curve of \mathcal{S} to the axis circle of revolution. Then:*

- \mathcal{S} has index at least $\max(5, 2k + 1)$.
- If \mathcal{S} is nodoidal with $k \geq 2$, then \mathcal{S} has index at least $\max(11, 2k + 5)$.
- If \mathcal{S} is unduloidal with $w \geq 2$, then \mathcal{S} has index at least $\max(6w - 1, 2k + 4w - 3)$.

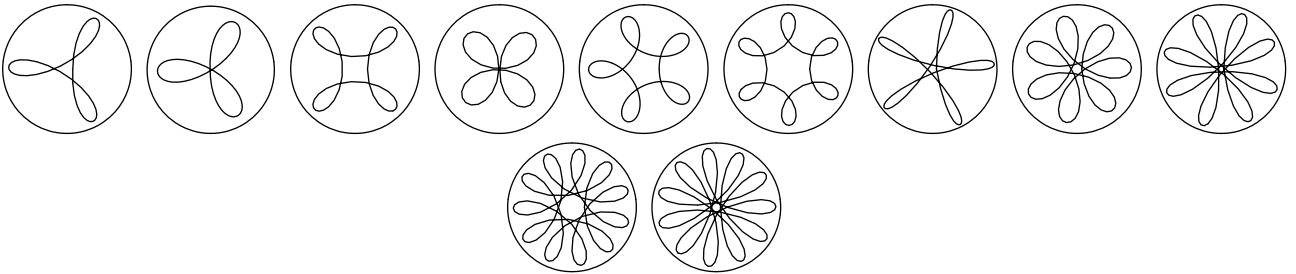


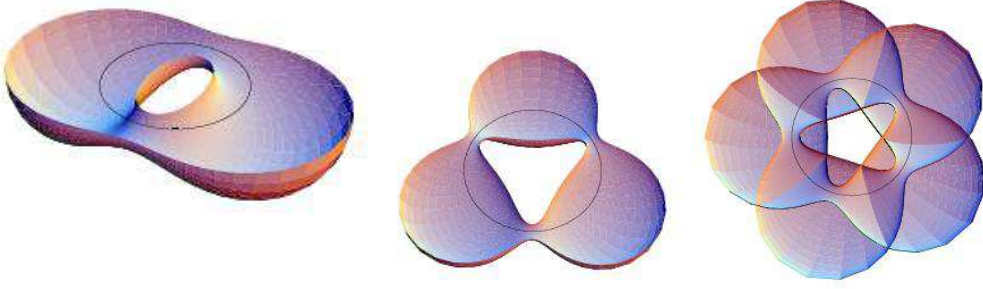
FIGURE 2. Profile curves for surfaces that we label N_i for $i = 1, 2, \dots, 11$ (N_1, \dots, N_9 from left to right in the upper row, N_{10}, N_{11} from left to right in the lower row). All of these surfaces are nodoidal, i.e. they are not unduloidal.

The numerical results here show the lower bounds in the above theorem are very close to the true value for the Morse index in the case of unduloids. For example, using Table 1 and Lemma 4.2, the numerically computed index of the unduloid U_1 (resp. U_2, U_3, \dots, U_{17}) is 6 (resp. 8, 10, 12, 14, 12, 16, 20, 24, 20, 24, 32, 28, 32, 36, 36, 44), while the above theorem gives the lower bound 5 (resp. 7, 9, 11, 13, 11, 15, 19, 23, 19, 23, 31, 27, 31, 35, 35, 43) for the index. In all cases, the lower bound in Theorem 1.3 differs from the numerically computed value for the index by only 1, thus the lower bound is quite sharp.

The lower bounds in Theorem 1.3 are not as sharp in the case of nodoids, but still are greater than half of the numerically computed value for all of the surfaces shown in Figure 2. The numerically computed index of the nodoid N_1 (resp. N_2, N_3, \dots, N_{11}) is 12 (resp. 12, 18, 18, 24, 30, 20, 32, 34, 52, 48), while the above theorem gives the lower bound 11 (resp. 11, 13, 13, 15, 17, 15, 19, 21, 27, 27) for the index.

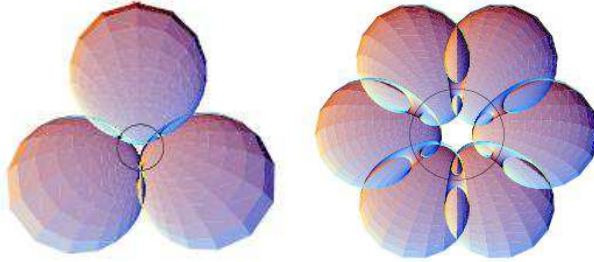
2. Proofs of the Theorems 1.1 and 1.2.

To prove Theorems 1.1 and 1.2, we give a series of lemmas. We first note that:

FIGURE 3. Half of each of the surfaces U_1, U_2, U_7 .

- For each λ , it is easily shown that the space of solutions of (1.1) amongst functions $f : \mathbb{R} \rightarrow \mathbb{R}$ is 2-dimensional.
- Consider the eigenvalue problem (1.1) over the function space \mathcal{F}_0 on the interval Σ_0 with Dirichlet boundary conditions. Suppose \hat{f}_1 and \hat{f}_2 are two linearly independent eigenfunctions corresponding to some eigenvalue λ . Noting that $(\frac{d}{dx}\hat{f}_1)(0)$ and $(\frac{d}{dx}\hat{f}_2)(0)$ are both nonzero, take the linear combination $\hat{f}_3 = (\frac{d}{dx}\hat{f}_2)(0) \cdot \hat{f}_1 - (\frac{d}{dx}\hat{f}_1)(0) \cdot \hat{f}_2$. Then $\hat{f}_3(0) = (\frac{d}{dx}\hat{f}_3)(0) = 0$, and it follows that \hat{f}_3 is identically zero, contradicting the linear independence of \hat{f}_1 and \hat{f}_2 . Hence the eigenvalues are simple. Hence the eigenvalues are always simple for the Dirichlet eigenvalue problem. Furthermore, multiplying by a scalar factor if necessary, we may assume the initial conditions for an eigenfunction f is $f(0) = 0$ and $(\frac{d}{dx}f)(0) = 1$.

For the closed eigenvalue problem (1.1) with $f \in \mathcal{F}_p$, the eigenspace associated to any eigenvalue λ is either 1 or 2 dimensional, and we have the following lemma regarding the initial conditions to find a basis for the eigenspace:

FIGURE 4. Half of each of the surfaces N_1, N_6 .

Lemma 2.1. *Suppose $V \in \mathcal{F}_p$ has the symmetry (1.2). Let $\lambda_1 < \lambda_2 \leq \lambda_3 \leq \dots \uparrow +\infty$ be the spectrum of \mathcal{L} over the space \mathcal{F}_p with a corresponding basis f_1, f_2, f_3, \dots of eigenfunctions. Then the eigenspaces are each at most 2-dimensional, and to find a basis for $\{f \in \mathcal{F}_p \mid \mathcal{L}(f) = \lambda_j f\}$ for some eigenvalue λ_j , we may assume:*

- When the eigenspace for λ_j is 1-dimensional, we may take a single eigenfunction $f_j \in \mathcal{F}_p$ such that

$$\text{either } f_j(0) = 1, \left(\frac{d}{dx}f_j\right)(0) = 0 \text{ or } f_j(0) = 0, \left(\frac{d}{dx}f_j\right)(0) = 1.$$

- When the eigenspace for $\lambda_j = \lambda_{j+1}$ is 2-dimensional, we may take two eigenfunctions $f_j, f_{j+1} \in \mathcal{F}_p$ such that

$$f_j(0) = 1, \left(\frac{d}{dx}f_j\right)(0) = 0 \text{ and } f_{j+1}(0) = 0, \left(\frac{d}{dx}f_{j+1}\right)(0) = 1.$$

Proof. First we consider the case of a 1-dimensional eigenspace. Let $f_j \in \mathcal{F}_p$ be a basis element of this eigenspace. If f_j has neither the symmetry $f_j(x) = f_j(-x)$ nor $f_j(-x) = -f_j(x)$, then $f_j(x)$ and $f_j(-x)$ would be two linearly independent eigenfunctions with eigenvalue λ_j , a contradiction. Hence $f_j(x) = f_j(-x)$ or $f_j(-x) = -f_j(x)$ for all $x \in \mathbb{R}$, and so $f_j(0) = 0$ or $(\frac{d}{dx}f_j)(0) = 0$. Furthermore, because multiplying f_j by a real constant still gives a solution to (1.1) with $\lambda = \lambda_j$, we may assume either $f_j(0) = 1$ or $(\frac{d}{dx}f_j)(0) = 1$. Hence the first part of the lemma is shown.

For the case of a 2-dimensional eigenspace, any C^∞ solution $f : \mathbb{R} \rightarrow \mathbb{R}$ to (1.1) with $\lambda = \lambda_j$ lies in \mathcal{F}_p , hence we can choose a basis $f_j, f_{j+1} \in \mathcal{F}_p$ with the initial conditions as in the second part of the lemma. \square

The following lemma is known as Courant's nodal domain theorem, and the proof, which applies in our setting with either function space \mathcal{F}_p or \mathcal{F}_0 , can be found in [4] (see also [15]).

Lemma 2.2. (Courant's nodal domain theorem.) *The number of nodes of any eigenfunction for (1.1) in \mathcal{F}_p (resp. \mathcal{F}_0) associated to the j 'th eigenvalue λ_j is at most j (resp. $j + 1$).*

Lemma 2.2 may be strengthened using Sturm comparison, as we will see in the course of proving Theorems 1.1 and 1.2.

The following lemma is a slight generalization of a result in [8]:

Lemma 2.3. *Consider the following two equations*

$$(2.1) \quad \frac{d^2}{dx^2}f + (V + \lambda)f = 0, \quad \frac{d^2}{dx^2}\hat{f} + (V + \hat{\lambda})\hat{f} = 0$$

with V as in (1.1) and $\lambda < \hat{\lambda}$. Suppose that the first equation in (2.1) has a solution $f(x) \not\equiv 0$ having two consecutive zeros at $x = \xi_1$ and $x = \xi_2$, with $\xi_1 < \xi_2$. Let $\hat{f}(x)$ be a solution of the second equation in (2.1), then $\hat{f}(x)$ has at least one zero $x = \xi_3$ with $\xi_1 < \xi_3 < \xi_2$.

Proof. Multiplying the first equation in (2.1) by \hat{f} and the second equation in (2.1) by f , then subtracting the first expression from the second and integrating, we have

$$(2.2) \quad \int_{\xi_1}^{\xi_2} (\hat{\lambda} - \lambda) f \hat{f} dx = \left[\left(\frac{d}{dx} f \right) \hat{f} - \left(\frac{d}{dx} \hat{f} \right) f \right]_{\xi_1}^{\xi_2} = \left(\frac{d}{dx} f \right) (\xi_2) \hat{f}(\xi_2) - \left(\frac{d}{dx} f \right) (\xi_1) \hat{f}(\xi_1),$$

as here $f(\xi_1) = f(\xi_2) = 0$. Multiplying by the scalar -1 if necessary, we may assume $f(x) > 0$ for $x \in (\xi_1, \xi_2)$, so $\left(\frac{d}{dx} f \right) (\xi_1) > 0$ and $\left(\frac{d}{dx} f \right) (\xi_2) < 0$. If $\hat{f}(x)$ is positive everywhere in (ξ_1, ξ_2) , then $\int_{\xi_1}^{\xi_2} (\hat{\lambda} - \lambda) f \hat{f} dx > 0$ and $\left(\frac{d}{dx} f \right) (\xi_2) \hat{f}(\xi_2) - \left(\frac{d}{dx} f \right) (\xi_1) \hat{f}(\xi_1) \leq 0$, contradicting (2.2). Similarly, $\hat{f}(x)$ cannot be negative everywhere in (ξ_1, ξ_2) . \square

Lemma 2.4. *Consider the eigenvalue problem (1.1) on \mathcal{F}_0 over the interval Σ_0 with Dirichlet boundary conditions, and with corresponding spectrum $\lambda_1 < \lambda_2 < \dots$ of simple eigenvalues. Then any eigenfunction associated with λ_j has exactly $j + 1$ nodes.*

Proof. Denote a nonzero eigenfunction corresponding to eigenvalue λ_j by f_j . Lemma 2.2 implies f_1 has exactly two nodes (at $x = 0$ and $x = a$). Assume f_j has exactly $j + 1$ nodal domains and let us prove f_{j+1} has exactly $j + 2$ nodes. From (1.1) we have $\frac{d^2}{dx^2}f_j + Vf_j + \lambda_j f_j = 0$ and $\frac{d^2}{dx^2}f_{j+1} + Vf_{j+1} + \lambda_{j+1}f_{j+1} = 0$. Let $\xi_1, \xi_2, \dots, \xi_{j-1}$ be the zeros of f_j in the interval $(0, a)$. Since $\lambda_{j+1} > \lambda_j$, applying Lemma 2.3, we conclude that f_{j+1} must vanish in each the intervals $(0, \xi_1), (\xi_1, \xi_2), \dots, (\xi_{j-1}, a)$ and hence that it has at least $j + 2$ nodes. Lemma 2.2 implies it has exactly $j + 2$ nodes. \square

The following lemma is proven in [8]:

Lemma 2.5. *Let f and \hat{f} be two linearly independent solutions of Equation (1.1) for the same λ , and suppose that f has two consecutive zeros ξ_1 and ξ_2 such that $\xi_1 < \xi_2$, then \hat{f} has one and only one zero in (ξ_1, ξ_2) .*

Proof. We may assume f is positive for all $x \in (\xi_1, \xi_2)$, then we have $\left(\frac{d}{dx} f \right) (\xi_1) > 0$ and $\left(\frac{d}{dx} f \right) (\xi_2) < 0$. Because f and \hat{f} are independent, $\hat{f}(\xi_k) \neq 0$ for $k = 1, 2$. Here $\frac{d}{dx} \left(\left(\frac{d}{dx} \hat{f} \right) f - \left(\frac{d}{dx} f \right) \hat{f} \right) = 0$ for all x , so $\left(\frac{d}{dx} f \right) (\xi_1) \hat{f}(\xi_1) = \left(\frac{d}{dx} f \right) (\xi_2) \hat{f}(\xi_2)$. Hence \hat{f} cannot keep a constant sign throughout the interval (ξ_1, ξ_2) , i.e. \hat{f} has at least one zero in (ξ_1, ξ_2) .

Now suppose η_1 and η_2 are two zeros of \hat{f} in (ξ_1, ξ_2) . If we interchange the roles of f and \hat{f} in the above argument, we conclude that f has at least one zero in (η_1, η_2) , a contradiction. Hence \hat{f} has exactly one zero in (ξ_1, ξ_2) . \square

Lemma 2.6. *Any two eigenfunctions of (1.1) in \mathcal{F}_p associated with equal eigenvalues have the same number of nodes.*

Proof. Let f and \hat{f} be two eigenfunctions associated with $\lambda_j = \lambda_{j+1}$ in the spectrum of \mathcal{L} over \mathcal{F}_p . If f and \hat{f} are linearly dependent, then the lemma clearly holds, so we assume they are linearly independent.

Suppose f has k nodes $\xi_1, \xi_2, \dots, \xi_k \in [0, a)$. Then $\hat{f}(\xi_\ell) \neq 0$ for $\ell = 1, \dots, k$, and by Lemma 2.5, \hat{f} has a unique node in each of $(\xi_1, \xi_2), (\xi_2, \xi_3), \dots, (\xi_{k-1}, \xi_k)$ and $(\xi_k, \xi_1 + a)$. Hence \hat{f} has exactly k nodes. \square

Lemma 2.7. *Take λ_j as in Theorem (1.2). Let f_j and f_k in \mathcal{F}_p be two eigenfunctions of \mathcal{L} corresponding to eigenvalues λ_j and λ_k with $\lambda_j < \lambda_k$, and with either of the initial conditions as in Lemma (2.1). Let n_j and n_k denote the number of nodes in Σ_p of f_j and f_k , respectively. If f_j and f_k have the same initial conditions, resp. different initial conditions, then $n_k \geq n_j + 2$, resp. $n_k \geq n_j$.*

Proof. Suppose $f_j(0) = f_k(0) = 0$, $(\frac{d}{dx}f_j)(0) = (\frac{d}{dx}f_k)(0) = 1$. So f_j has $n_j - 1$ nodes between $x = 0$ and $x = a$. Then by Lemma 2.3, f_k has at least n_j nodes in the open interval $(0, a)$, and so $n_k > n_j$. Since n_j and n_k are both even, $n_k \geq n_j + 2$.

Now suppose $f_j(0) = f_k(0) = 1$, $(\frac{d}{dx}f_j)(0) = (\frac{d}{dx}f_k)(0) = 0$, then f_j has n_j nodes ξ_1, \dots, ξ_j in the open interval $(0, a)$. Also, f_j and f_k have the symmetry $f_j(x) = f_j(-x)$ and $f_k(x) = f_k(-x)$ for all $x \in [0, a]$, by the symmetry (1.2). By Lemma 2.3, f_k has a node in each interval $(\xi_\ell, \xi_{\ell+1})$ for $\ell = 1, \dots, n_j - 1$. Also, it has a node in $(-\xi_1, \xi_1)$, so by the above symmetry, it has at least two nodes in $(-\xi_1, \xi_1)$, implying $n_k > n_j$ and so $n_k \geq n_j + 2$.

If f_j and f_k have different initial conditions, then Lemma 2.3 immediately implies $n_k \geq n_j$. \square

Lemma 2.8. *Take λ_j as in Theorem (1.2). Let f_{j-1} , f_j and f_{j+1} in \mathcal{F}_p be three consecutive eigenfunctions associated with λ_{j-1} , λ_j and λ_{j+1} , respectively, each with either of the initial conditions as in Lemma (2.1). Let n_{j-1} , n_j and n_{j+1} denote the number of nodes of f_{j-1} , f_j and f_{j+1} respectively. Then $n_{j+1} \geq n_{j-1} + 2$.*

Proof. Here each of the eigenfunctions f_{j-1} , f_j and f_{j+1} has either of the two initial conditions given in Lemma (2.1). Thus two of these functions will have the same initial conditions, hence by Lemma 2.7 we have at least one of $n_j \geq n_{j-1} + 2$ or $n_{j+1} \geq n_{j-1} + 2$ or $n_{j+1} \geq n_j + 2$. Lemma 2.7 also implies $n_{j-1} \leq n_j \leq n_{j+1}$, hence the result is shown. \square

All of the lemmas in this section (Section 2) immediately imply Theorems 1.1 and 1.2.

3. Computation of the spectrum of \mathcal{L} over \mathcal{F}_p with symmetric V

A numerical method for computing the spectrum of \mathcal{L} on the function space \mathcal{F}_p is as follows:

- (1) The eigenfunctions are in \mathcal{F}_p and so are periodic, and the real-analytic $V \in \mathcal{F}_p$ is assumed to have the symmetry (1.2). Theorem 1.2 implies we can numerically solve (1.1) for f with the initial conditions just either $f(0) = 1$, $(\frac{d}{dx}f)(0) = 0$ or $f(0) = 0$, $(\frac{d}{dx}f)(0) = 1$ by a numerical ODE solver, and search for the values of λ that give periodic solutions f , i.e. give $f \in \mathcal{F}_p$. Such values of λ are amongst the λ_j .
- (2) By Theorem 1.2, we know the eigenspaces are at most 2-dimensional. If, for some $\lambda = \lambda_j$, one of the two types of initial conditions in Theorem 1.2 for f gives a solution $f \in \mathcal{F}_p$ and the other does not, then the eigenspace of λ_j is 1-dimensional; if both types of initial conditions give solutions $f \in \mathcal{F}_p$, then the eigenspace of λ_j is 2-dimensional.
- (3) From Theorem 1.2, we know that any eigenfunction f associated to λ_j has exactly j nodes when j is even, and $j - 1$ nodes otherwise. So the value of j is determined simply by counting the number of nodes of f . Because we can determine j , we will know when we have found all $\lambda_j \leq M$ for any given $M \in \mathbb{R}$.

4. Application to CMC surfaces of revolution in \mathbb{S}^3

As an application of the numerical approach described in Section 3, we consider CMC tori of revolution in the unit 3-sphere $\mathbb{S}^3 \subset \mathbb{R}^4$ and compute the spectra of their Jacobi operators. This gives us a numerical evaluation of the Morse index of these surfaces.

Let $\mathcal{S}(x, y) : \mathcal{T} = \{(x, y) \in \mathbb{R}^2 \mid (x, y) \equiv (x + a, y) \equiv (x, y + 2\pi)\} \rightarrow \mathbb{S}^3$ be a conformal immersion from the torus \mathcal{T} to \mathbb{S}^3 , with mean curvature H and Gauss curvature K . When H is constant, \mathcal{S} is critical for a variation problem whose associated *Jacobi operator* is

$$-\Delta - \hat{V} \quad \text{with} \quad \hat{V} = 4 + 4H^2 - 2K,$$

where Δ is the Laplace-Beltrami operator of the induced metric $ds^2 = g(dx^2 + dy^2)$ for some smooth function $g = g(x, y)$ (g is in fact real-analytic in the application here). We take \mathcal{S} to be a non-flat CMC torus of revolution.

Let us define

$$\mathcal{L} = -g\Delta - g\hat{V} = \frac{\partial^2}{\partial x^2} - \frac{\partial^2}{\partial y^2} - V,$$

where $V = g\hat{V}$. Then the eigenvalues of \mathcal{L} form a discrete sequence whose corresponding eigenfunctions can be chosen to form an orthonormal basis for the L^2 norm over \mathcal{T} with respect to the Euclidean metric $dx^2 + dy^2$. Let

$$\lambda_1 < \lambda_2 \leq \lambda_3 \leq \dots \uparrow +\infty$$

be the spectrum of \mathcal{L} .

By using Rayleigh quotient characterizations for eigenvalues it can be shown that \mathcal{L} and $-\Delta - \hat{V}$ will give the same number of negative eigenvalues (counted with multiplicity), although these two operators will have different eigenvalues. Hence we can use either \mathcal{L} or $-\Delta - \hat{V}$ to find the Morse index of the surface \mathcal{S} :

surface	nonpositive eigenvalues $\lambda_{1,0}, \lambda_{2,0}, \dots, \lambda_{k,0}$ (where $\lambda_{k,0} = 0$ and $\lambda_{k+1,0} > 0$), for the operator $\hat{\mathcal{L}}$
U_1	-1.28, -1, -1, -0.25, 0
U_2	-1.08, -1, -1, -0.76, -0.76, -0.51, 0
U_3	-1.04, -1, -1, -0.87, -0.87, -0.67, -0.67, -0.52, 0
U_4	-1.03, -1, -1, -0.91, -0.91, -0.78, -0.78, -0.6, -0.6, -0.48, 0
U_5	-1.02, -1, -1, -0.94, -0.94, -0.84, -0.84, -0.714, -0.714, -0.57, -0.57, -0.48, 0
U_6	-1.64, -1.48, -1.48, -1, -1, -0.36, 0
U_7	-1.13, -1.1, -1.1, -1, -1, -0.84, -0.84, -0.64, -0.64, -0.5, 0
U_8	-1.05, -1.04, -1.04, -1, -1, -0.94, -0.94, -0.86, -0.86, -0.77, -0.77, -0.68, -0.68, -0.64, 0
U_9	-1.029, -1.022, -1.022, -1, -1, -0.96, -0.96, -0.92, -0.92, -0.86, -0.86, -0.79, -0.79, -0.72, -0.72, -0.66, -0.66, -0.63, 0
U_{10}	-1.28, -1.25, -1.25, -1.15, -1.15, -1, -1, -0.83, -0.83, -0.72, 0
U_{11}	-1.11, -1.1, -1.1, -1.06, -1.06, -1, -1, -0.92, -0.92, -0.83, -0.83, -0.75, -0.75, -0.71, 0
U_{12}	-1.04, -1.03, -1.03, -1.02, -1.02, -1, -1, -0.97, -0.97, -0.94, -0.94, -0.896, -0.896, -0.85, -0.85, -0.8, -0.8, -0.76, -0.76, -0.73, -0.73, -0.72, 0
U_{13}	-1.14, -1.13, -1.13, -1.1, -1.1, -1.06, -1.06, -1, -1, -0.94, -0.94, -0.88, -0.88, -0.86, 0
U_{14}	-1.14, -1.13, -1.13, -1.1, -1.1, -1.06, -1.06, -1, -1, -0.93, -0.93, -0.84, -0.84, -0.75, -0.75, -0.67, -0.67, -0.63, 0
U_{15}	-1.07, -1.06, -1.06, -1.05, -1.05, -1.03, -1.03, -1, -1, -0.96, -0.96, -0.92, -0.92, -0.87, -0.87, -0.83, -0.83, -0.78, -0.78, -0.75, -0.75, -0.74, 0
U_{16}	-1.11, -1.1, -1.1, -1.09, -1.09, -1.07, -1.07, -1.04, -1.04, -1, -1, -0.96, -0.96, -0.93, -0.93, -0.9, -0.9, -0.89, 0
U_{17}	-1.26, -1.25, -1.25, -1.23, -1.23, -1.19, -1.19, -1.14, -1.14, -1.08, -1.08, -1, -1, -0.91, -0.91, -0.81, -0.81, -0.71, -0.71, -0.62, -0.62, -0.59, 0
N_1	-1.26, -1.19, -1.19, -1, -1, -0.85, 0
N_2	-1.42, -1.31, -1.31, -1, -1, -0.696, 0
N_3	-1.43, -1.37, -1.37, -1.22, -1.22, -1, -1, -0.85, 0
N_4	-1.85, -1.76, -1.76, -1.47, -1.47, -1, -1, -0.55, 0
N_5	-1.67, -1.62, -1.62, -1.49, -1.49, -1.27, -1.27, -1, -1, -0.83, 0
N_6	-1.7, -1.67, -1.67, -1.58, -1.58, -1.43, -1.43, -1.22, -1.22, -1, -1, -0.88, 0
N_7	-1.09, -1.08, -1.08, -1.05, -1.05, -1, -1, -0.95, -0.95, -0.93, 0
N_8	-1.47, -1.45, -1.45, -1.39, -1.39, -1.29, -1.29, -1.16, -1.16, -1, -1, -0.84, -0.84, -0.75, 0
N_9	-1.18, -1.176, -1.176, -1.15, -1.15, -1.11, -1.11, -1.06, -1.06, -1, -1, -0.94, -0.94, -0.89, -0.89, -0.87, 0
N_{10}	-1.31, -1.3, -1.3, -1.29, -1.29, -1.26, -1.26, -1.22, -1.22, -1.18, -1.18, -1.12, -1.12, -1.06, -1.06, -1, -1, -0.94, -0.94, -0.9, -0.9, -0.89, 0
N_{11}	-1.19, -1.18, -1.18, -1.17, -1.17, -1.15, -1.15, -1.12, -1.12, -1.09, -1.09, -1.05, -1.05, -1, -1, -0.95, -0.95, -0.91, -0.91, -0.89, -0.89, -0.88, 0

TABLE 1. Numerical estimates for the nonpositive eigenvalues of the operator $\hat{\mathcal{L}}$ for the specific examples of CMC non-flat tori of revolution shown in Figures 1 and 2. The values are rounded off to the nearest hundredth or thousandth.

Definition 4.1. The *Morse index* $\text{Ind}(\mathcal{S})$ of \mathcal{S} is the sum of multiplicities of the negative eigenvalues of $-\Delta - \hat{V}$ with function space the smooth functions from \mathcal{T} to \mathbb{R} . Equivalently, it is the sum of the multiplicities of the negative eigenvalues of \mathcal{L} over the same function space.

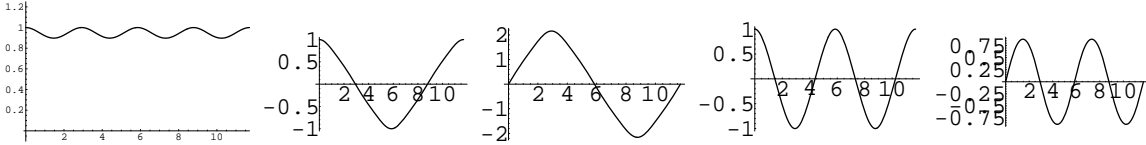


FIGURE 5. Eigenfunctions associated to the eigenvalues $\lambda_{1,0}, \dots, \lambda_{4,0}, \lambda_{5,0} = 0$ of the surface U_1 .

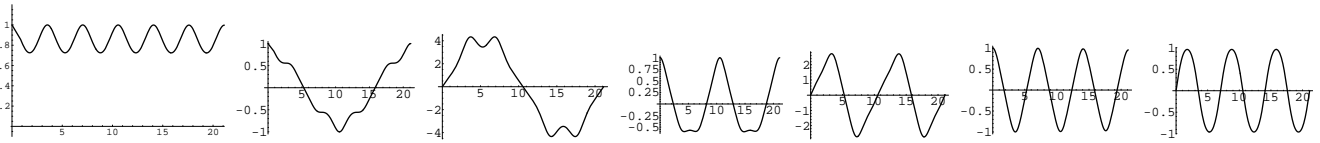


FIGURE 6. Eigenfunctions associated to the eigenvalues $\lambda_{1,0}, \dots, \lambda_{6,0}, \lambda_{7,0} = 0$ of the surface U_2 .

A C^∞ function $f = f(x, y) : \mathcal{T} \rightarrow \mathbb{R}$ can be decomposed into a series of spherical harmonics as follows:

$$(4.1) \quad f = \sum_{j=0}^{\infty} u_{j,1}(x) \cos(jy) + u_{j,2}(x) \sin(jy),$$

where $u_{j,1}, u_{j,2} \in \mathcal{F}_p$ for Σ_p with the given $a > 0$. The operator $\hat{\mathcal{L}}$ on the function space \mathcal{F}_p is defined by

$$\hat{\mathcal{L}} = -\frac{d^2}{dx^2} - V,$$

and the spectrum

$$\lambda_{1,0} < \lambda_{2,0} \leq \lambda_{3,0} \leq \dots \uparrow +\infty$$

surface \mathcal{S}	s	t	a	k	w	\mathcal{B}_1	\mathcal{B}_2	\mathcal{B}_3	numerical value for $\text{Ind}(\mathcal{S})$
U_1	0.4078	0.1583	11.7053	2	1	0	1	1	6
U_2	0.4392	0.0812	21.1215	3	1	0	1	3	8
U_3	0.4352	0.0758	28.9593	4	1	0	1	5	10
U_4	0.4275	0.0796	36.0835	5	1	0	1	7	12
U_5	0.4259	0.0789	43.5185	6	1	0	1	9	14
U_6	0.4703	0.1697	15.6572	3	2	0	3	1	12
U_7	0.4431	0.0881	34.0978	5	2	0	3	5	16
U_8	0.4561	0.0559	53.6192	7	2	0	3	9	20
U_9	0.4526	0.0545	69.8309	9	2	0	3	13	24
U_{10}	0.4949	0.0707	33.7818	5	3	0	5	3	20
U_{11}	0.4738	0.0528	53.0235	7	3	0	5	7	24
U_{12}	0.4667	0.0426	89.2538	11	3	0	5	15	32
U_{13}	0.4987	0.0354	56.6566	7	4	0	7	5	28
U_{14}	0.4659	0.0675	64.3347	9	4	0	7	9	32
U_{15}	0.47302	0.0438	87.7273	11	4	0	7	13	36
U_{16}	0.4993	0.0269	77.7075	9	5	0	9	7	36
U_{17}	0.4719	0.0893	71.551	11	6	0	11	9	44
N_1	0.5112	-0.0502	21.7946	3	1	0	3	1	12
N_2	0.5061	-0.089	18.6334	3	1	0	3	1	12
N_3	0.5292	-0.068	26.0688	4	1	0	5	1	18
N_4	0.5257	-0.155	20.1429	4	1	0	5	1	18
N_5	0.5501	-0.095	28.6743	5	1	0	7	1	24
N_6	0.56002	-0.092	34.3367	6	1	0	9	1	30
N_7	0.5027	-0.0197	46.0084	5	2	0	5	3	20
N_8	0.5199	-0.087	43.0143	7	2	0	9	3	32
N_9	0.5047	-0.039	62.452	8	3	0	9	5	34
N_{10}	0.5211	-0.051	78.4551	11	3	0	15	5	52
N_{11}	0.5064	-0.039	86.0723	11	4	0	13	7	48

TABLE 2. Here \mathcal{B}_1 is the number of eigenvalues less than -4 , \mathcal{B}_2 is the number of eigenvalues in $[-4, -1)$, and \mathcal{B}_3 is the number of eigenvalues in $(-1, 0)$, all counted with multiplicity.

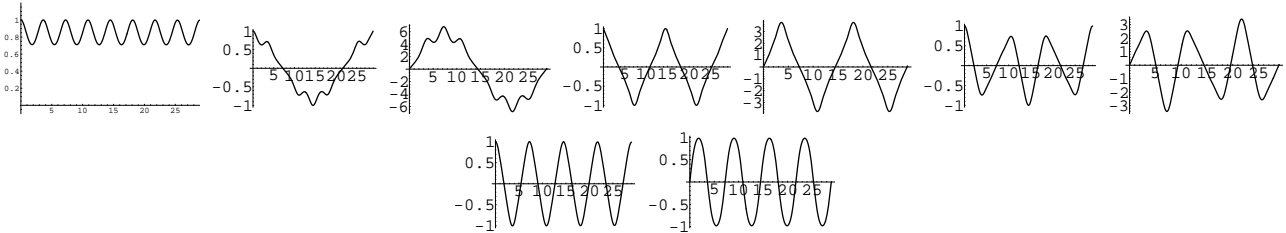
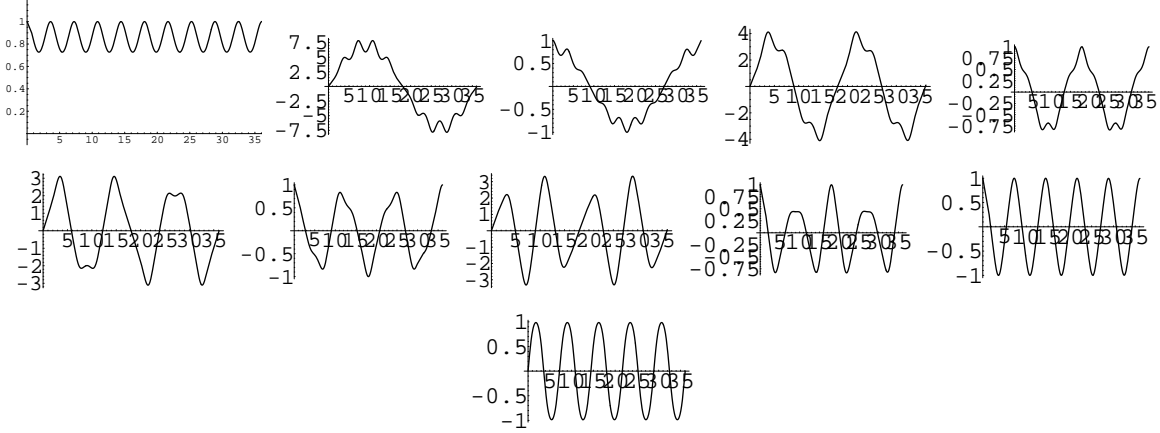
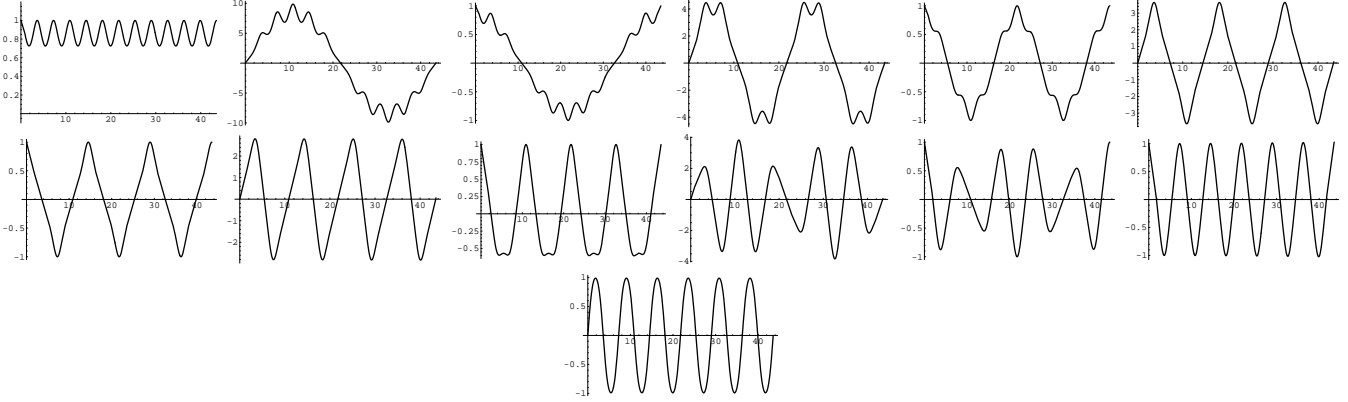
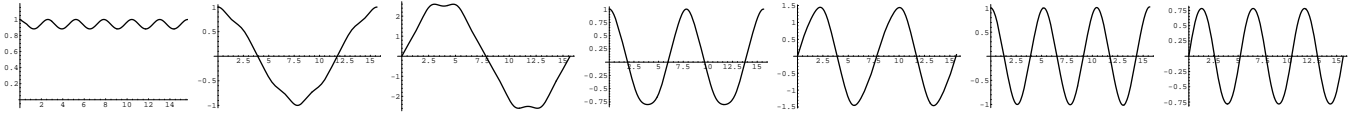


FIGURE 7. Eigenfunctions associated to the eigenvalues $\lambda_{1,0}, \dots, \lambda_{8,0}, \lambda_{9,0} = 0$ of the surface U_3 .

of $\hat{\mathcal{L}}$ has all the analogous properties as those of the spectrum for \mathcal{L} . Furthermore, by uniqueness of the spherical harmonics decomposition, f is an eigenfunction of \mathcal{L} for the eigenvalue λ if and only if each $u_{j,k}$, $k = 1, 2$, is an eigenfunction of $\hat{\mathcal{L}}$ for the eigenvalue $\lambda - j^2$. And if f is not identically zero, then some $u_{j,k}$ will also be not identically zero. Thus we can say:

- λ is an eigenvalue for the operator \mathcal{L} if and only if $\lambda - n^2$ is an eigenvalue for the operator $\hat{\mathcal{L}}$ for some $n \in \mathbb{N} \cup \{0\}$.


 FIGURE 8. Eigenfunctions associated to the eigenvalues $\lambda_{1,0}, \dots, \lambda_{10,0}, \lambda_{11,0} = 0$ of the surface U_4 .

 FIGURE 9. Eigenfunctions associated to the eigenvalues $\lambda_{1,0}, \dots, \lambda_{12,0}, \lambda_{13,0} = 0$ of the surface U_5 .

 FIGURE 10. Eigenfunctions associated to the eigenvalues $\lambda_{1,0}, \dots, \lambda_{6,0}, \lambda_{7,0} = 0$ of the surface U_6 .

- For any eigenvalue $\lambda_{j,0} < -n^2$, $n \in \mathbb{N} \cap [2, \infty)$, of $\hat{\mathcal{L}}$, with associated eigenfunction $f_j \in \mathcal{F}_p$, the eigenvalues of \mathcal{L} associated to the eigenfunctions $f_j \cdot \cos(ky)$ and $f_j \cdot \sin(ky)$, for integers $k \leq [0, n]$, will be negative.

Furthermore, we can conclude the following:

Lemma 4.2. *We have*

$$\text{Ind}(\mathcal{S}) = \sum_{j \in \mathbb{N}} \lambda_{j,0} \cdot \ell(\lambda_{j,0}), \quad \text{where } \ell(\lambda) = \begin{cases} 0 & \text{if } \lambda \geq 0, \\ 2i - 1 & \text{if } \lambda \in [-i^2, -(i-1)^2] \text{ for } i \in \mathbb{N}. \end{cases}$$

Proof. Let $E(\lambda)$, resp. $E_0(\lambda)$, denote the eigenspace of solutions of $\mathcal{L}(f) = \lambda f$ for smooth $f : \mathcal{T} \rightarrow \mathbb{R}$, resp. $\hat{\mathcal{L}}(f) = \lambda f$ for $f \in \mathcal{F}_p$. Then $\dim E(\lambda) = 0$, resp. $\dim E_0(\lambda) = 0$ whenever λ is not an eigenvalue of \mathcal{L} , resp. $\hat{\mathcal{L}}$, and is a positive integer otherwise. Then, by the uniqueness of the spherical harmonics decomposition,

$$\sum_{\lambda < 0} \dim E(\lambda) = \sum_{\lambda < 0} \left(\dim E_0(\lambda) + 2 \sum_{j \geq 1} \dim E_0(\lambda - j^2) \right) = \left(\sum_{\lambda < 0} \dim E_0(\lambda) \right) + 2 \sum_{j \geq 1} \sum_{\lambda < -j^2} \dim E_0(\lambda).$$

□

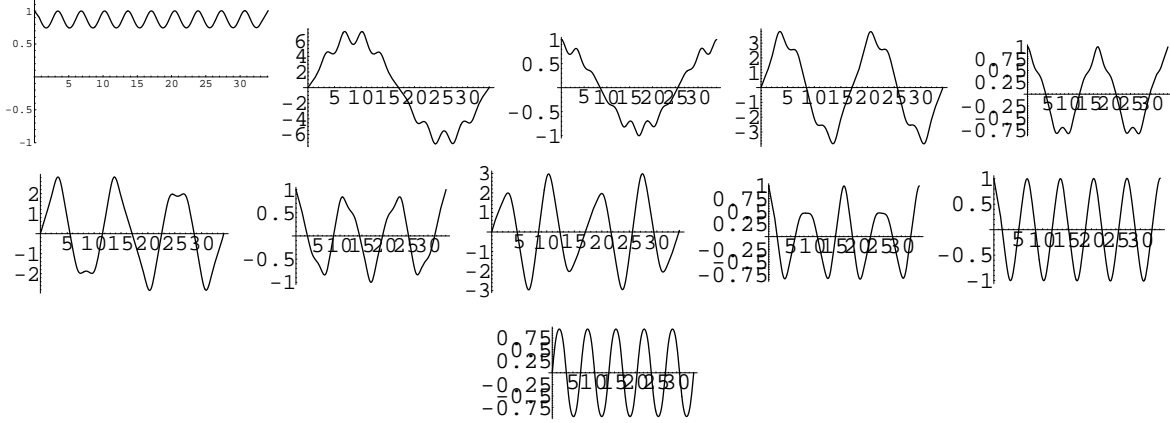


FIGURE 11. Eigenfunctions associated to the eigenvalues $\lambda_{1,0}, \dots, \lambda_{10,0}, \lambda_{11,0} = 0$ of the surface U_7 .

Here \mathcal{S} is a CMC surface of revolution, so, following [16], we can consider

$$\mathcal{L} = -\frac{\partial^2}{\partial x^2} - \frac{\partial^2}{\partial y^2} - 2v^2 - 32s^2t^2v^{-2} \quad \text{and} \quad \hat{\mathcal{L}} = -\frac{d^2}{dx^2} - 2v^2 - 32s^2t^2v^{-2},$$

where $s \in \mathbb{R}^+$, $t \in (-s, s) \setminus \{0\}$, $\gamma \in (0, \pi/4]$, and s, t, γ (we note that $\cot(2\gamma)$ is the mean curvature of \mathcal{S}) satisfy the conditions $(s+t)^2 - 4st \sin^2 \gamma = 1/4$ and

$$st \in (-(16 \sin^2 \gamma)^{-1}, 0) \cup (0, (16 \cos^2 \gamma)^{-1}),$$

and $v = v(x)$ is the elliptic function

$$v = \frac{2t}{\operatorname{dn}_\tau(2sx)} \quad \text{with period} \quad x_0 = \frac{1}{s} \int_0^1 \frac{d\rho}{\sqrt{(1-\rho^2)(1-\tau^2\rho^2)}}, \quad \text{where} \quad \tau = \sqrt{1-t^2/s^2}.$$

When $st > 0$, we have unduloidal surfaces. When $st < 0$, we have either nodoidal or unduloidal surfaces (see [16]).

Using the method in Section 3, we can numerically compute the negative eigenvalues of $\hat{\mathcal{L}}$, and can then apply Lemma 4.2 to find $\operatorname{Ind}(\mathcal{S})$. We do this for the CMC tori of revolution shown in Figures 1 and 2. In [16], it is shown that 0 is an eigenvalue of $\hat{\mathcal{L}}$, and -1 is an eigenvalue of $\hat{\mathcal{L}}$ with multiplicity 2. Since $\ell(\lambda)$ is discontinuous at $\lambda = 0$ and $\lambda = -1$, it is crucial to know that both 0 and -1 are eigenvalues of $\hat{\mathcal{L}}$ in order to determine $\operatorname{Ind}(\mathcal{S})$. Furthermore, as the eigenvalue -1 has multiplicity 2 and $\lambda_{1,0}$ must be simple, we have $\lambda_{1,0} < -1$. (In the numerical experiments here, we find that 0 is always a simple eigenvalue.)

Tables 1, 2 and Figures 5-32 show results of our numerical computations.

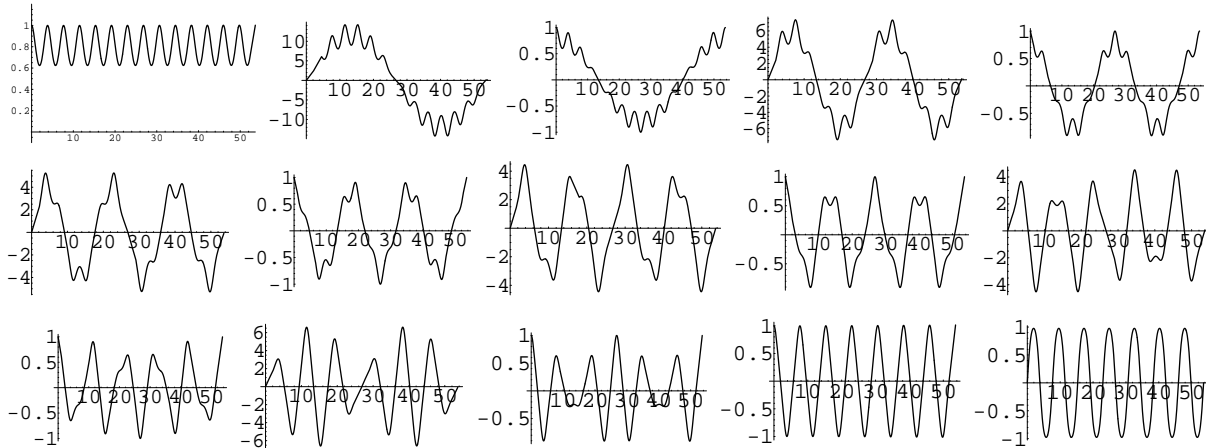


FIGURE 12. Eigenfunctions associated to the eigenvalues $\lambda_{1,0}, \dots, \lambda_{14,0}, \lambda_{15,0} = 0$ of the surface U_8 .

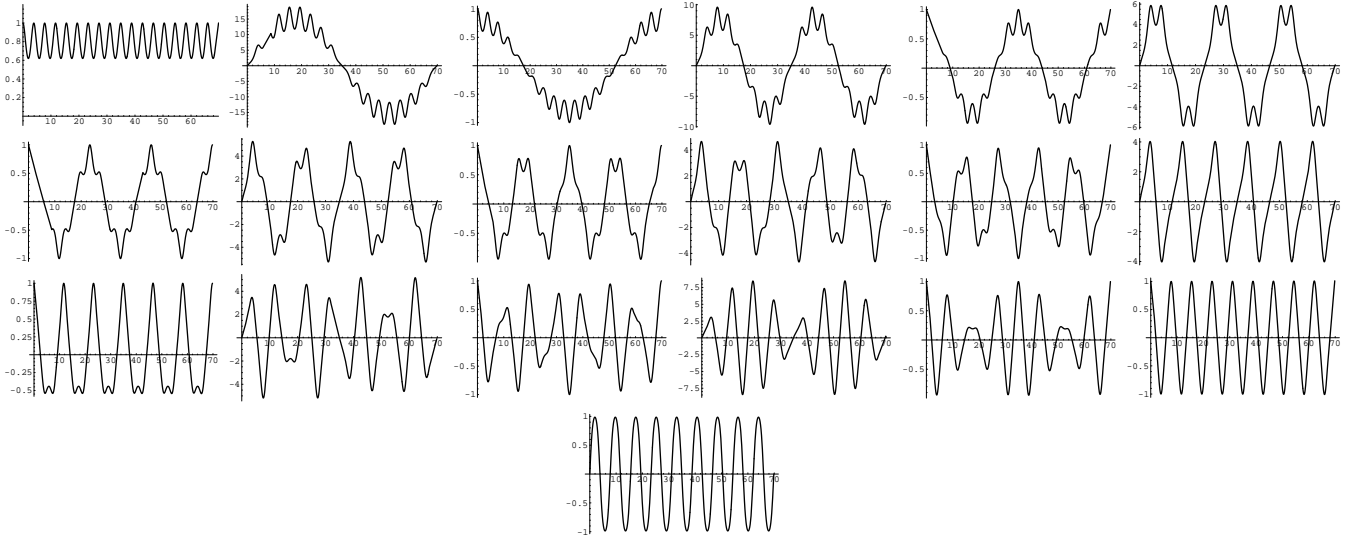


FIGURE 13. Eigenfunctions associated to the eigenvalues $\lambda_{1,0}, \dots, \lambda_{18,0}, \lambda_{19,0} = 0$ of the surface U_9 .

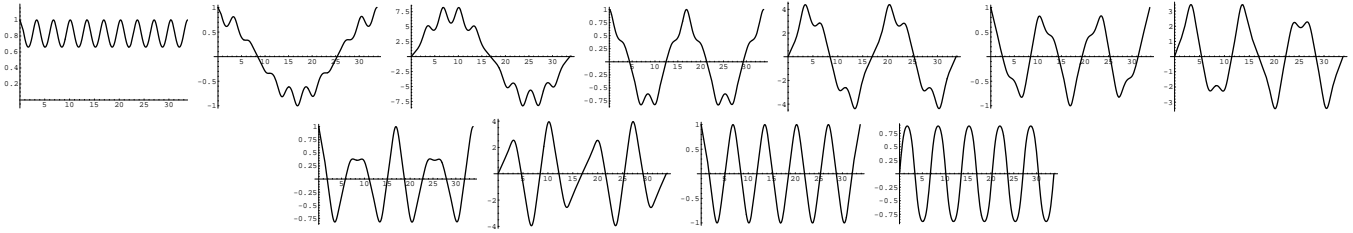


FIGURE 14. Eigenfunctions associated to the eigenvalues $\lambda_{1,0}, \dots, \lambda_{10,0}, \lambda_{11,0} = 0$ of the surface U_{10} .

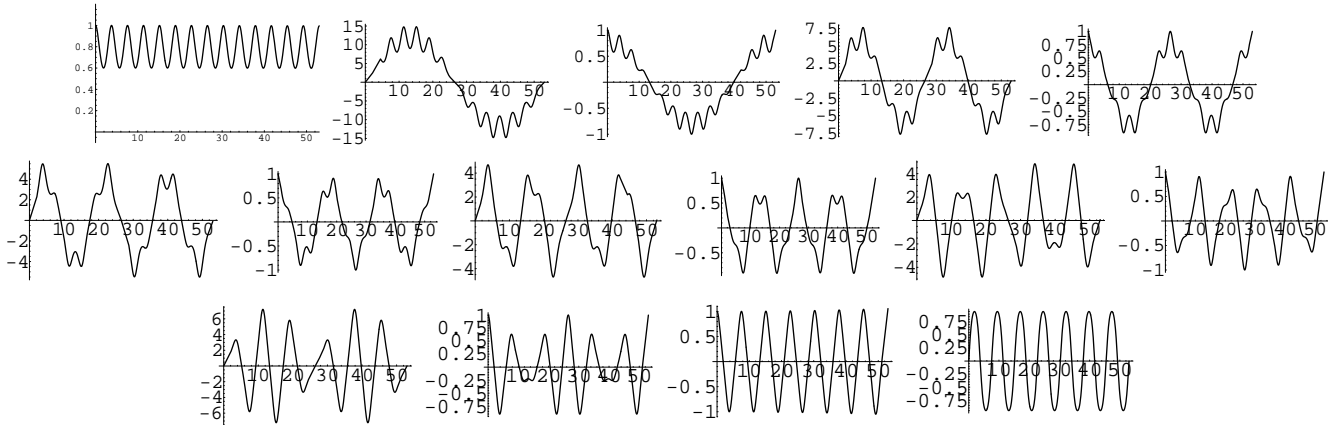


FIGURE 15. Eigenfunctions associated to the eigenvalues $\lambda_{1,0}, \dots, \lambda_{14,0}, \lambda_{15,0} = 0$ of the surface U_{11} .

REFERENCES

- [1] L. Barbosa, M. do Carmo and J. Eschenburg, *Stability of hypersurfaces of constant mean curvature in Riemannian manifolds*, Math. Z. 197 (1988), 123-138.
- [2] P. Berard, *Spectral Geometry: Direct and Inverse Problems*, Lecture notes in Mathematics 1207 (1986).
- [3] M. Berger, P. Gauduchon, E. Mazet, *Le Spectre d'une Variete Riemannienne*, Lecture Notes in Math. 194 (1971).
- [4] S.-Y. Cheng, *Eigenfunctions and nodal sets*, Comment. Math. Helvetici 51 (1976), 43-55.
- [5] R. Courant and D. Hilbert, *Methods of mathematical physics*, Volume I, Interscience publishers, Inc., New York, 1937.
- [6] J. Diedonne, *Foundation of Mathematical Analysis*, Academic Press, 1960.

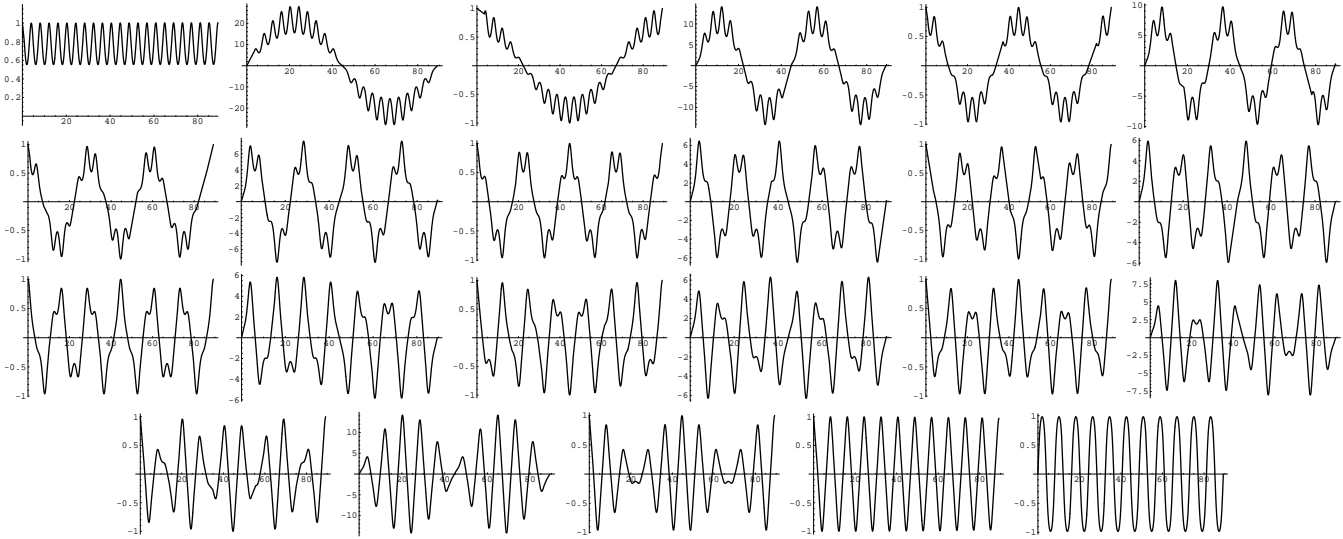


FIGURE 16. Eigenfunctions associated to the eigenvalues $\lambda_{1,0}, \dots, \lambda_{22,0}, \lambda_{23,0} = 0$ of the surface U_{12} .

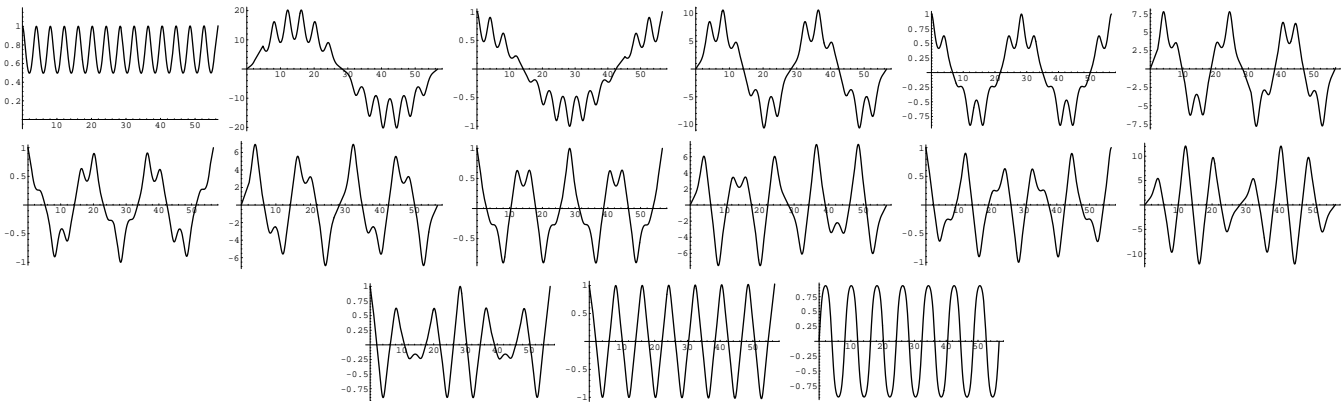


FIGURE 17. Eigenfunctions associated to the eigenvalues $\lambda_{1,0}, \dots, \lambda_{14,0}, \lambda_{15,0} = 0$ of the surface U_{13} .

- [7] P. Hartman, *Ordinary differential equations*, John Wiley and Sons, Inc., 1964.
- [8] E. Hille, *Lectures on ordinary differential equations*, Addison-Wesley publishing company, 1969.
- [9] W. Y. Hsiang, *On generalization of theorems of A. D. Alexandrov and C. Delaunay on hypersurfaces of constant mean curvature*, Duke Math. J. 49(3) (1982), 485-496.
- [10] W. Y. Hsiang and W. C. Yu, *A generalization of a theorem of Delaunay*, J. Diff. Geom. 16 (1981), 161-177.
- [11] H. B. Lawson Jr., *Complete minimal surfaces in S^3* , Ann. of Math. 92(2) (1970), 335-374.
- [12] S. G. Mikhailin, *Variational methods in mathematical physics*, Pergamon Press (1964).
- [13] W. Rossman, *The Morse index of Wente tori*, Geometriae Dedicata 86 (2001), 129-151.
- [14] W. Rossman, *The first bifurcation point for Delaunay nodoids*, J. Exp. Math. 14(3) (2005), 331-342.
- [15] W. Rossman, *Lower bounds for Morse index of constant mean curvature tori*, Bull. London Math. Soc. 34 (2002), 599-609.
- [16] W. Rossman and N. Sultana, *Morse index of constant mean curvature tori of revolution in the 3-sphere*, preprint, arXiv:math.DG/0605127.
- [17] N. Schmitt, M. Kilian, S-P. Kobayashi, W. Rossman, *Constant mean curvature surfaces with Delaunay ends in 3-dimensional space forms*, to appear in J. London Math. Soc.
- [18] N. Sultana, *Explicit parametrization of Delaunay surfaces in space forms via loop group methods*, Kobe Journal of Mathematics Vol. 22, No. 1-2 (2005).
- [19] H. Urakawa, *Geometry of Laplace-Beltrami operator on a complete Riemannian manifold*, Progress on Diff. Geometry, Adv. Stud. Pure Math. 22 (1993), 347-406.

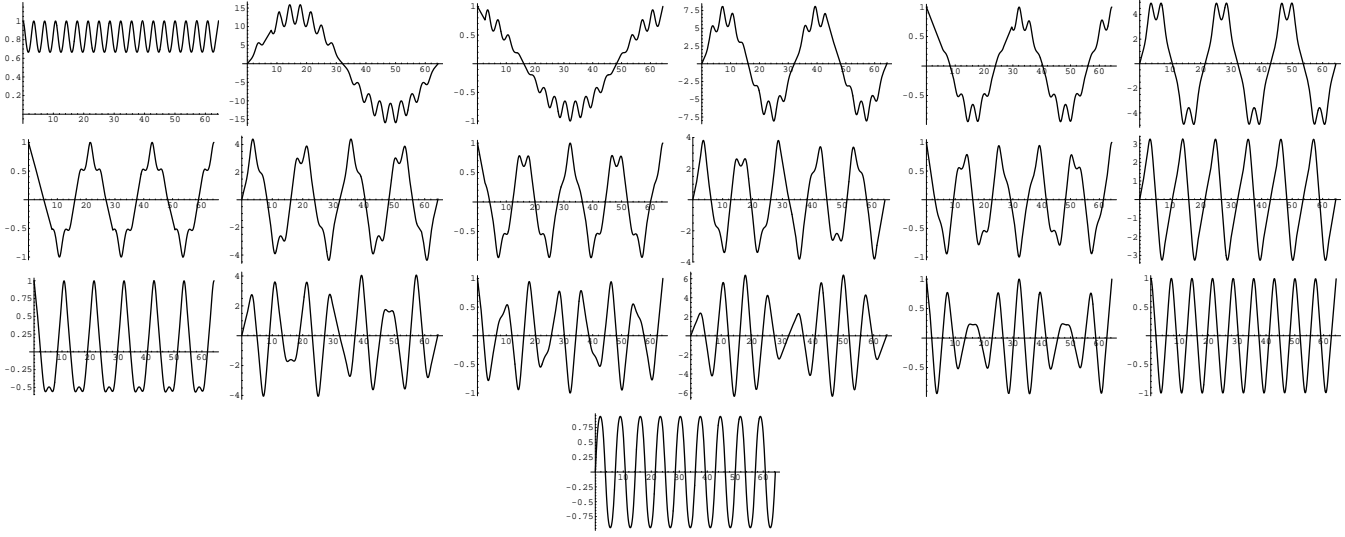


FIGURE 18. Eigenfunctions associated to the eigenvalues $\lambda_{1,0}, \dots, \lambda_{18,0}, \lambda_{19,0} = 0$ of the surface U_{14} .

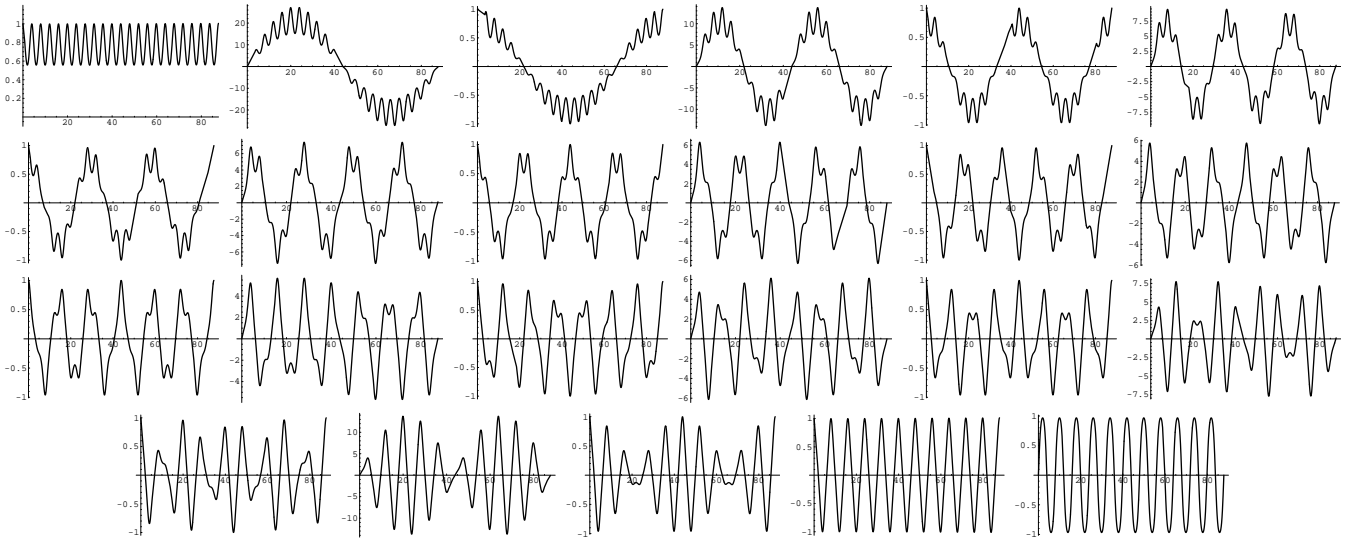


FIGURE 19. Eigenfunctions associated to the eigenvalues $\lambda_{1,0}, \dots, \lambda_{22,0}, \lambda_{23,0} = 0$ of the surface U_{15} .

DEPARTMENT OF MATHEMATICS, KOBE UNIVERSITY, KOBE 657-8501, JAPAN
E-mail address: wayne@math.kobe-u.ac.jp

DEPARTMENT OF MATHEMATICS, KOBE UNIVERSITY, KOBE 657-8501, JAPAN
E-mail address: nahid@math.kobe-u.ac.jp

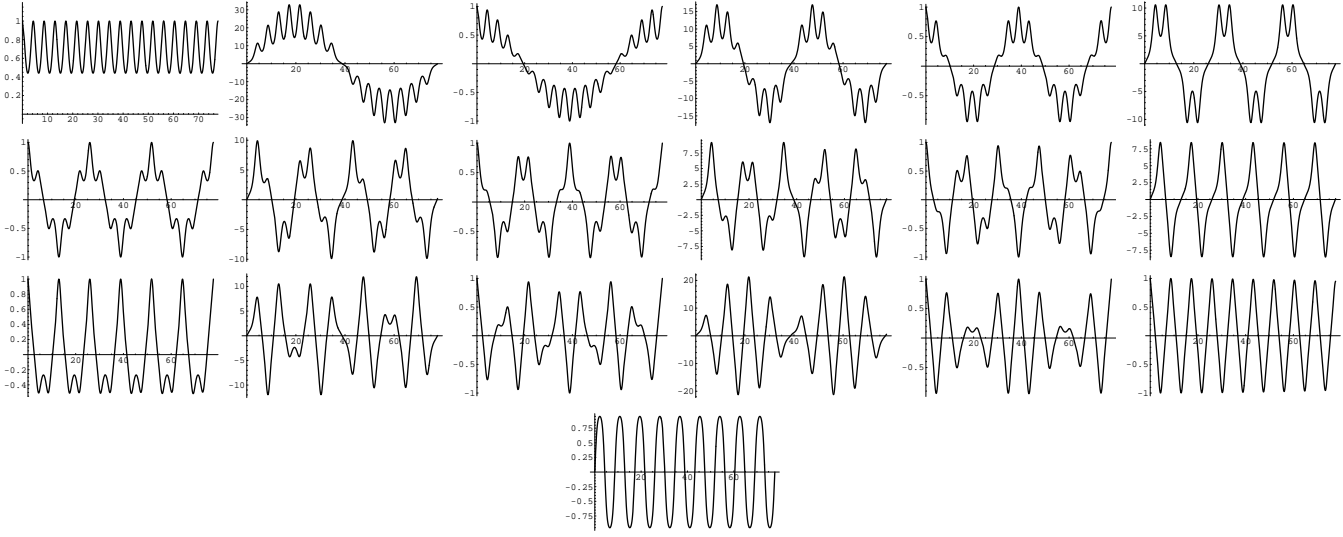


FIGURE 20. Eigenfunctions associated to the eigenvalues $\lambda_{1,0}, \dots, \lambda_{18,0}, \lambda_{19,0} = 0$ of the surface U_{16} .

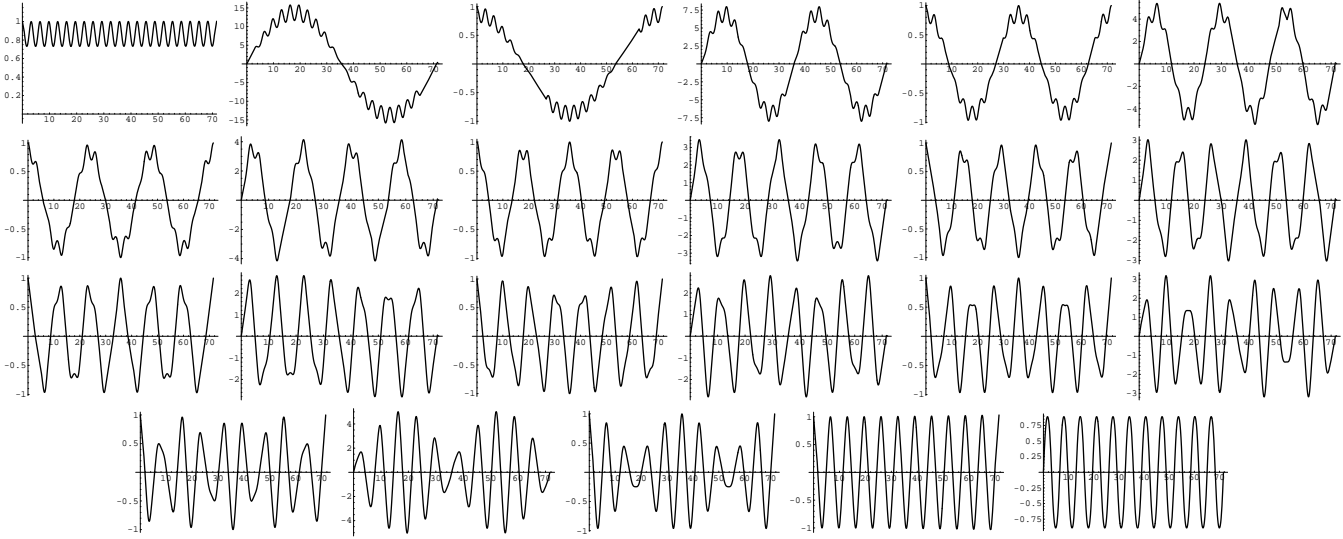


FIGURE 21. Eigenfunctions associated to the eigenvalues $\lambda_{1,0}, \dots, \lambda_{22,0}, \lambda_{23,0} = 0$ of the surface U_{17} .

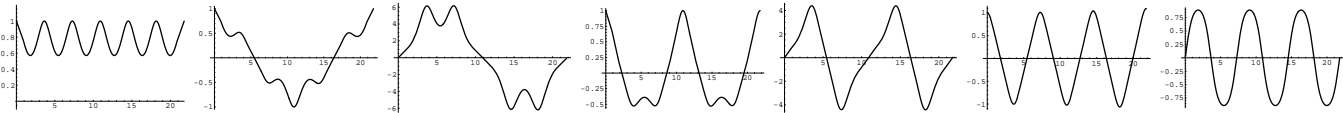


FIGURE 22. Eigenfunctions associated to the eigenvalues $\lambda_{1,0}, \dots, \lambda_{6,0}, \lambda_{7,0} = 0$ of the surface N_1 .

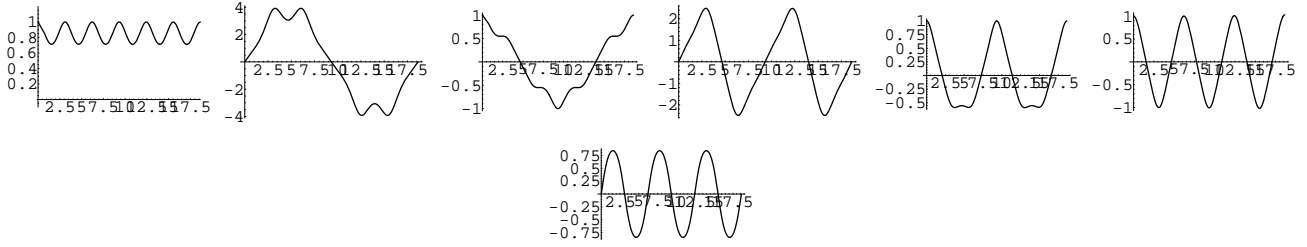


FIGURE 23. Eigenfunctions associated to the eigenvalues $\lambda_{1,0}, \dots, \lambda_{6,0}, \lambda_{7,0} = 0$ of the surface N_2 .

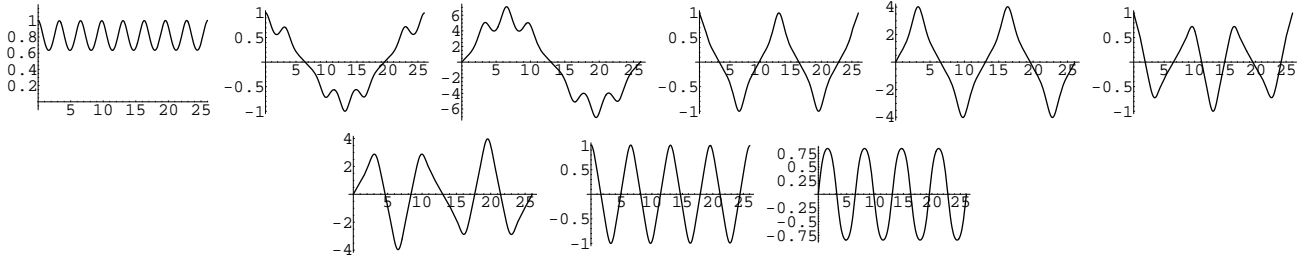


FIGURE 24. Eigenfunctions associated to the eigenvalues $\lambda_{1,0}, \dots, \lambda_{8,0}, \lambda_{9,0} = 0$ of the surface N_3 .

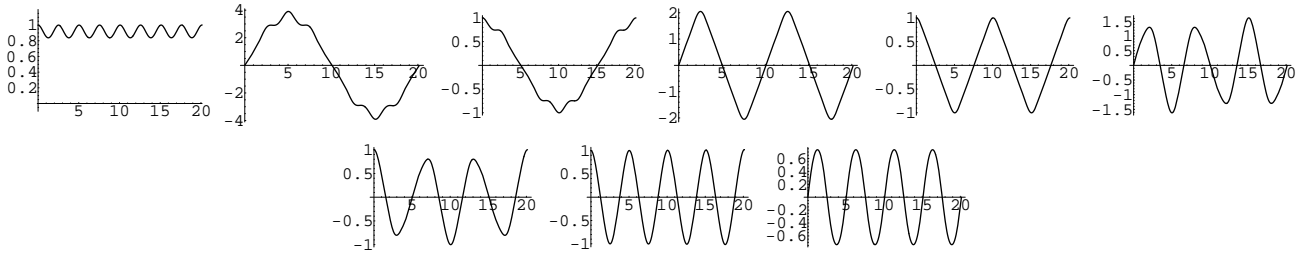


FIGURE 25. Eigenfunctions associated to the eigenvalues $\lambda_{1,0}, \dots, \lambda_{8,0}, \lambda_{9,0} = 0$ of the surface N_4 .

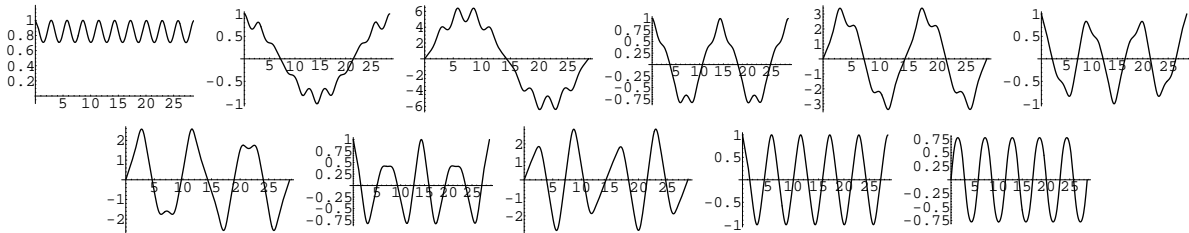


FIGURE 26. Eigenfunctions associated to the eigenvalues $\lambda_{1,0}, \dots, \lambda_{10,0}, \lambda_{11,0} = 0$ of the surface N_5 .

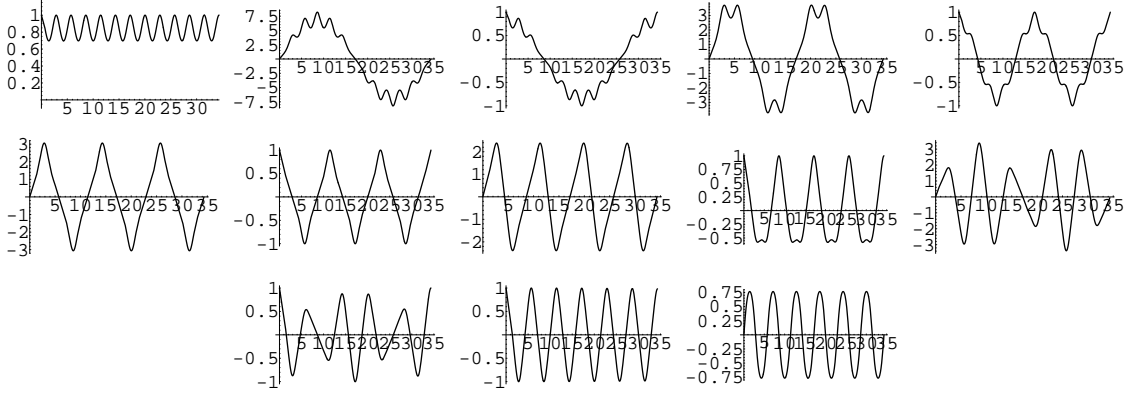


FIGURE 27. Eigenfunctions associated to the eigenvalues $\lambda_{1,0}, \dots, \lambda_{12,0}, \lambda_{13,0} = 0$ of the surface N_6 .

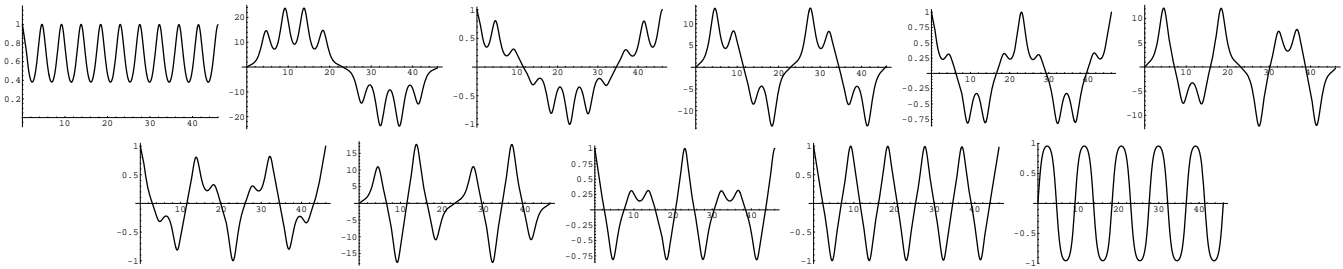


FIGURE 28. Eigenfunctions associated to the eigenvalues $\lambda_{1,0}, \dots, \lambda_{10,0}, \lambda_{11,0} = 0$ of the surface N_7 .

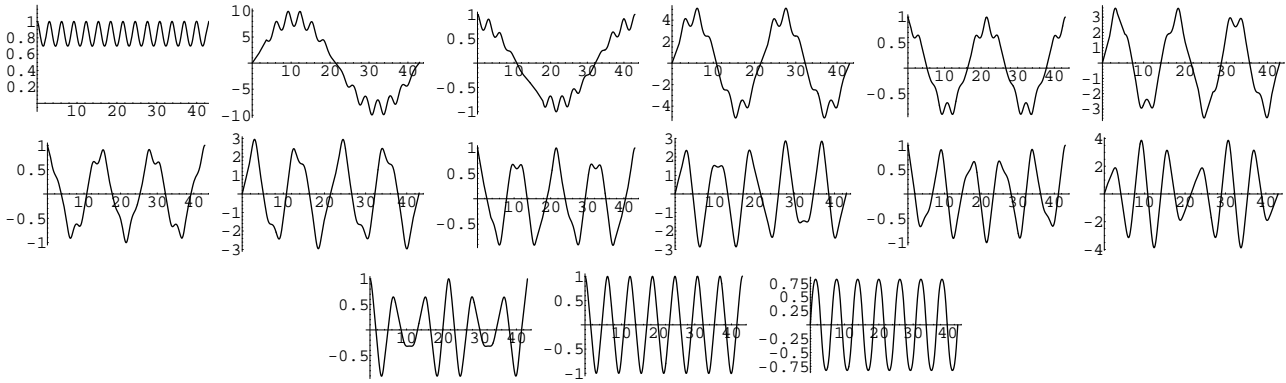


FIGURE 29. Eigenfunctions associated to the eigenvalues $\lambda_{1,0}, \dots, \lambda_{14,0}, \lambda_{15,0} = 0$ of the surface N_8 .

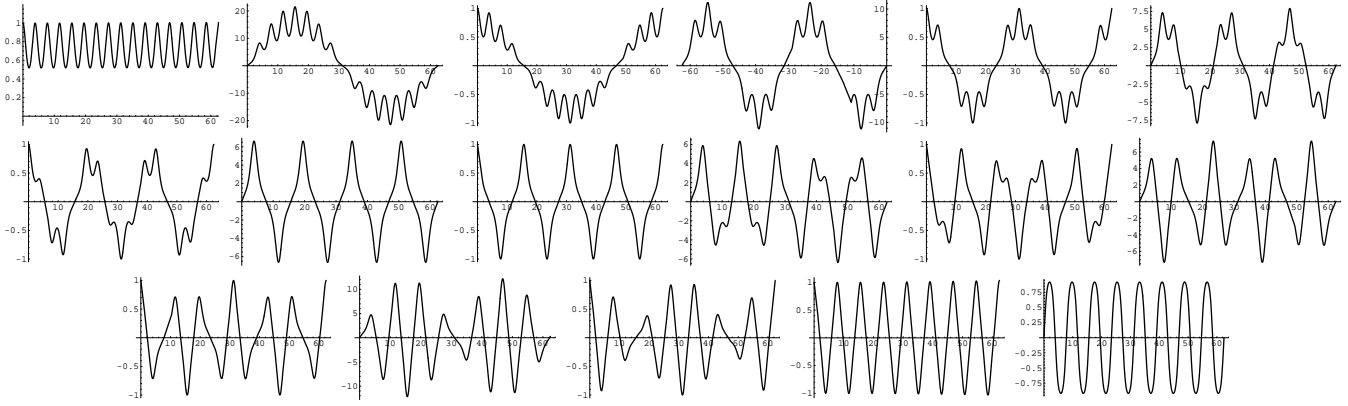


FIGURE 30. Eigenfunctions associated to the eigenvalues $\lambda_{1,0}, \dots, \lambda_{16,0}, \lambda_{17,0} = 0$ of the surface N_9 .

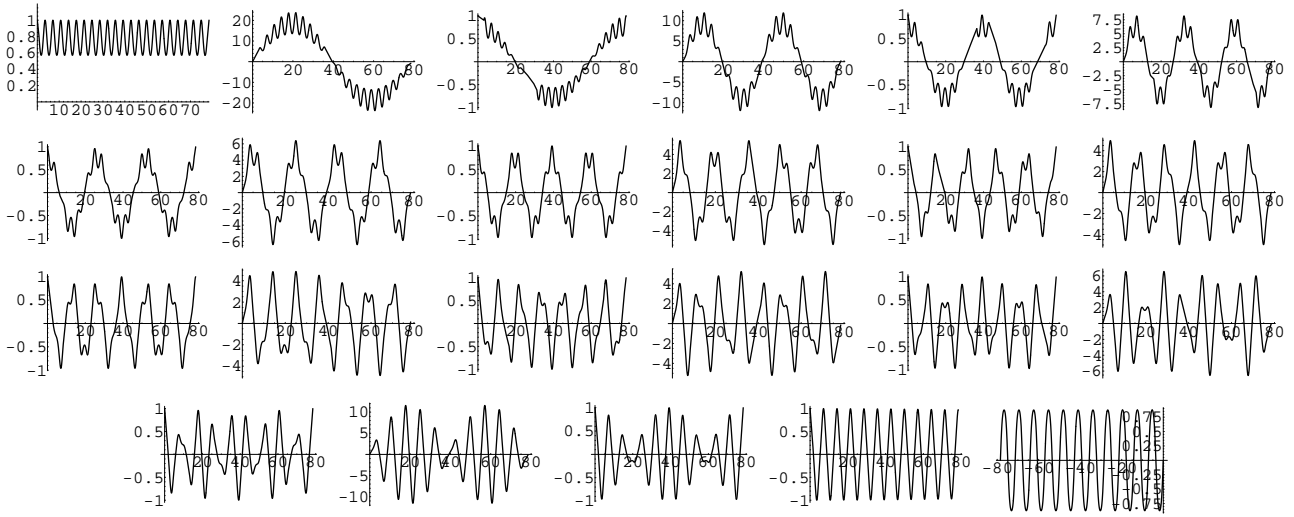


FIGURE 31. Eigenfunctions associated to the eigenvalues $\lambda_{1,0}, \dots, \lambda_{22,0}, \lambda_{23,0} = 0$ of the surface N_{10} .

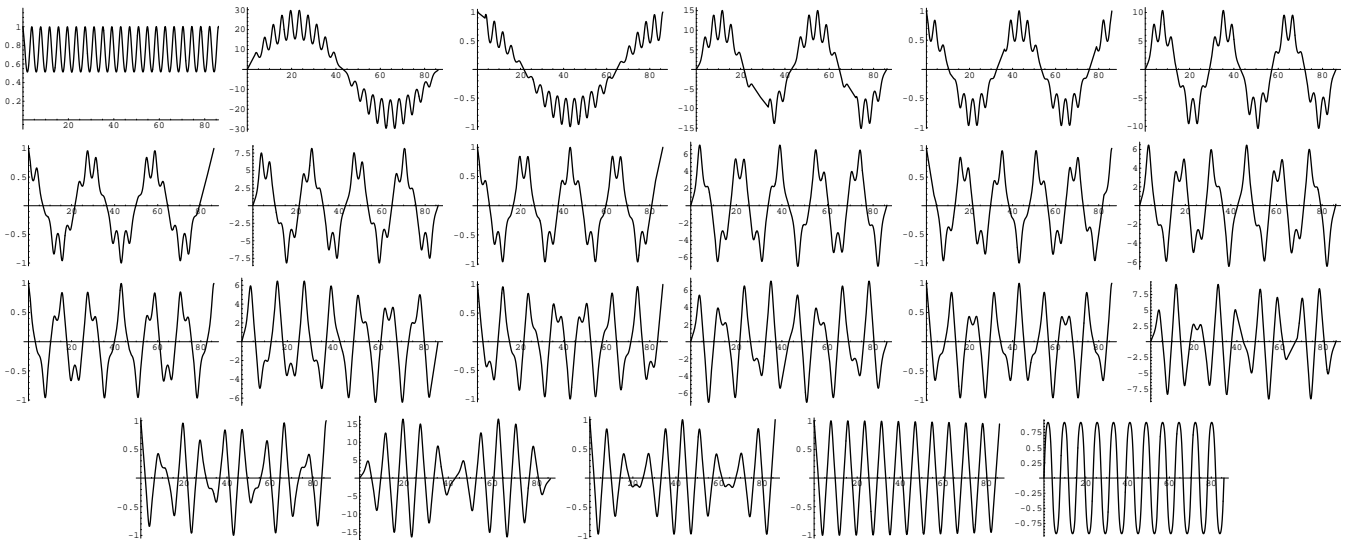


FIGURE 32. Eigenfunctions associated to the eigenvalues $\lambda_{1,0}, \dots, \lambda_{22,0}, \lambda_{23,0} = 0$ of the surface N_{11} .